

Hydrogen-Vacancy-Dislocation Interactions in α -Fe

A. Tehranchi^a, X. Zhang^b, G. Lu^b, W. A. Curtin^a

^aLaboratory for Multiscale Mechanics Modeling, EPFL, CH-1015 Lausanne, Switzerland

^bDepartment of Physics and Astronomy, California State University Northridge, Northridge, California 91330-8268, USA

Abstract. Atomistic simulations of the interactions between dislocations, hydrogen atoms, and vacancies are studied to assess the viability of a recently-proposed mechanism for the formation of nanoscale voids in Fe-based steels in the presence of hydrogen. QM/MM calculations confirm EAM simulations showing that individual vacancies on the compressive side of an edge dislocation can be transported with the dislocation as it glides. EAM simulations then show, however, that vacancy clusters in the glide plane of an approaching dislocation are annihilated or reduced in size by the creation of a double-jog/climb process that is driven by the huge reduction in energy accompanying vacancy annihilation. The effectiveness of annihilation/reduction processes is not reduced by the presence of hydrogen in the vacancy clusters since V-H cluster binding energies are much lower than the vacancy formation energy, except at very hydrogen content in the cluster. Analysis of a range of configurations indicates that Hydrogen plays no special role in stabilizing nanovoids. Experimental observations of nanovoids on the fracture surfaces of steels must be due to as-yet undetermined processes.

Keywords: Vacancy–Hydrogen cluster, DFT calculation, Jog formation, void growth

1. Introduction

Hydrogen embrittlement (HE) has been a persistent mode of degradation in metals in industrial applications for decades [1, 2, 3, 4]. Nonetheless, to date, the precise mechanisms for embrittlement remain far from understood at a mechanistic level, although many competing concepts have been proposed. These major concepts include hydrogen-enhanced decohesion (HEDE) [5, 6, 7, 8, 9, 10] and hydrogen-enhanced local plasticity (HELP) [11, 12, 13]. Hydrogen has many various observable effects in metals, for instance causing plastic softening or hardening, facilitating vacancy formation, segregating to dislocations and other traps, and segregating to grain boundaries with an associated reduction in the boundary cleavage energy. However, most of these phenomena do not have a direct mechanistic connection to embrittlement, i.e. a transition from high-toughness ductile-like failure to a much lower-toughness more-brittle like failure. One recent idea is that the transport and aggregation of H atoms to a crack tip inhibits dislocation emission, which prevents crack blunting, leaving cleavage as the only mechanism of reducing energy around the crack. Such a local “ductile-to-brittle” transition is driven by the prevention of ductile blunting processes rather than the decrease in cohesion energies [14, 15]. While this idea has found some quantitative success, it does not explain all observed features of embrittlement. Thus, hydrogen embrittlement, and its various manifestations in various metals remains an open general problem.

Recent experiments in Fe-based steels have revealed the presence of nanoscale voids on the grain boundary cleavage planes in the presence of hydrogen [16]. The precise role of the voids in facilitating crack growth is unclear, but mechanisms can be envisioned so that the mechanism(s) of nanovoid creation merits study. A potential mechanism explored in connection with these experiments posits that vacancy clusters form and are stabilized by the presence of hydrogen [16]. To support this idea, atomistic simulations based on Fe-H EAM potential were used to show that a single vacancy in bcc Fe can be transported by a single dislocation and then released when the vacancy encounters a hydrogen atom. A second vacancy swept into the same location was shown to lead to the formation of a two-vacancy/one-hydrogen cluster. From these two studies, and the knowledge that vacancy-hydrogen interactions in Fe (and many other metals) are attractive, such that the general reaction $nV + mH \rightarrow V_nH_m$ is energetically favorable, it was speculated that the observed nanovoid growth in steels is due to sequential vacancy sweeping by dislocations, trapping by hydrogen, and subsequent diffusion and coalescence of vacancies and voids [17]. These findings present an intriguing effect of Hydrogen that merits a more-complete study of the interactions among vacancies, hydrogen, and edge dislocations in bcc Fe.

Here, using a quantum-mechanics/molecular-mechanics method (QM/MM), we find that the configuration of a single vacancy in the Fe edge dislocation core differs from that predicted by the Fe EAM potential. However, both QM/MM and EAM based simulations predict that a single vacancy located on the compressive glide plane

of the dislocation can be transported with the dislocation as the dislocation glides. We then show, using the EAM potential that, when a gliding dislocation interacts with various vacancy/hydrogen clusters in the glide plane of the dislocation, the dislocation will annihilate vacancies and form jogs, leaving behind smaller or zero vacancy clusters in its wake. Most importantly, this process is largely independent of the presence of hydrogen. These processes are driven by the very large energy reduction associated with annihilating energetically-costly vacancies in Fe. Therefore, we conclude that neither dislocations nor hydrogen play any clearly positive role in the formation of vacancy clusters and, thus, that nanovoid formation by the processes envisioned in recent work is not operative. We discuss other possible mechanisms for the vacancy accumulation/void creation process that might be assisted by the presence of Hydrogen.

The remainder of this paper is organized as follows. In Section 2, we described the simulation details. In Section 3, we present important benchmark energies for various configurations involving vacancies, hydrogen atoms, and/or dislocations, as computed using QM/MM and/or the Fe-H EAM potential. In Section 4, we present results on the reactions of vacancies or vacancy clusters with edge dislocations in Fe, with and without hydrogen. In Section 5, we discuss our results and their implications for hydrogen-assisted nanovoid formation.

2. Simulation Details

For EAM simulations, which constitute the majority of the studies in this paper, we construct a rectangular simulation cell comprised of a bcc Fe crystal oriented with $X = [111]$, $Y = [1\bar{1}0]$ and $Z = [11\bar{2}]$, and of dimensions $L_x = 49.4\text{nm}$, $L_y = 14.6\text{nm}$ and $L_z = 28.0\text{nm}$ as illustrated in Figure 1. For problems involving a dislocation, we introduce a single edge dislocation of Burgers vector $1/2[111](1\bar{1}0)$ with line direction along Z and lying in the $Y=0$ plane. The edge dislocation is created by removing atoms from the perfect crystal in the narrow strip $-\sqrt{3}a_0/4 < X - X_0 < \sqrt{3}a_0/4$, $Y < 0$, where $a_0 = 2.86\text{\AA}$ is the lattice constant for α -Fe and X_0 is the X coordinate of the dislocation. All remaining atoms are then displaced according to the linear elastic displacement field for the edge dislocation [18], and the entire structure is relaxed using the conjugate gradient method [19]. The simulation cell is periodic along Z and along X, the latter introducing an artificial bending that does not, however, create any shear stress along the dislocation slip plane. Vacancies (V) are introduced at desired positions by removing the occupying Fe atom. H atoms are introduced by inserting them into the desired tetrahedral interstitial sites of the lattice or near-tetrahedral sites around vacancies. Various geometries are considered, as discussed below.

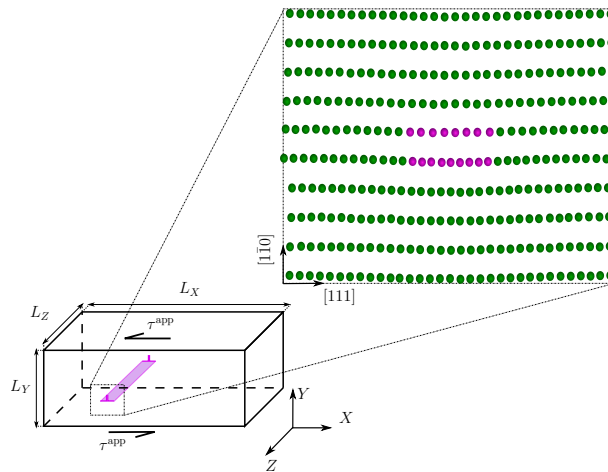


Figure 1: Schematic of the simulation cell used to study edge dislocation/vacancy/hydrogen interactions. Color coding uses due to Common Neighbor Analysis with green indicating a bcc environment and red indicating non-bcc environments.

To drive dislocation motion, the system is loaded by applied forces on the Y surfaces corresponding to a desired resolved shear stress. MD simulations are performed in an NVT ensemble with a Langevin thermostat [20] using the velocity-Verlet algorithm [21] with the integration time step of 1 fs. The temperature of the system is fixed at $10^{-3}K$, so that MD is very nearly equivalent to a steepest-descent minimization. The molecular dynamics simulations are performed using the Large-scale Atomic/Molecular Massively Parallel Simulator (LAMMPS) [22] and atomic configurations are visualized using the Open Visualization Tool (OVITO) [23].

Interatomic interactions among atoms are described using an embedded atom method (EAM) potential introduced by Ramasubramaniam et al. [24] and modified by Song and Curtin [15] to prevent unphysical H aggregation in single-crystal Fe. The Peierls stress required to initiate dislocation glide is computed as 100

MPa, and all simulations involving dislocation glide reported below are thus executed at stresses slightly above 100 MPa. The potential used in the simulations is essentially identical to that used in the recent study of V–H–dislocation interactions [17]. To assess the validity of this potential for our studies involving Fe, H, and V, we have made comparisons of various energies as well as the structure of the core of the dislocation with and without a vacancy with the energies and structures obtained via the quantum-mechanical/molecular-mechanics method (QM/MM) method. The QM/MM method is that developed by Lu et al. [25, 26, 27], which has previously been used to study interaction of hydrogen interstitials and dislocations in bcc Fe [28]. Stand-alone DFT studies for point defects (V and H) were also performed in $4 \times 4 \times 4$ cubic unit cells with periodic boundary conditions. All DFT calculations are implemented in VASP [29, 30] with the projector augmented wave pseudopotentials (PAW) [31]. The energy cut off for the plane wave basis is set to be 300 eV and a $3 \times 3 \times 3$ Monkhorst–Pack [32] k-point mesh is used. The exchange and correlation function is approximated by the Perdew–Burke–Ernzerhof generalized gradient approximation (PBE-GGA) [31]. In QM/MM calculations, the EAM potential of Fe proposed by Shastry and Farkas [33] is employed in the MM region. This potential is rescaled to give the same lattice parameter and bulk modulus as those of the DFT calculations. The entire QM/MM system size is $202\text{\AA} \times 202\text{\AA} \times 6.25\text{\AA}$ in [111], $[\bar{1}10]$ and $[\bar{1}\bar{1}2]$ directions. The dimensions of the QM region are $21\text{\AA} \times 10\text{\AA} \times 6.25\text{\AA}$. The k-point mesh of $1 \times 1 \times 5$ is used in the constrained DFT scheme.

3. Vacancy/Hydrogen/Dislocation interaction energies in Fe

A range of defect energies have been computed using DFT and/or QM/MM and using the EAM potential. The results are summarized in Table 1. The Vacancy formation energy in bulk bcc Fe is computed to be $E_V^f = 1.73\text{eV}$ for the EAM potential as compared to $E_V^f = 2.17\text{eV}$ as computed with QM/MM and also with standard periodic-cell DFT. The Vacancy/Hydrogen binding energy for VH_n clusters was reported previously [15] for $n=1-6$, with the EAM potential in generally good agreement with standard DFT studies. The difference between the binding energies calculated by DFT and EAM potential for all n except $n = 4$ were less than 0.05 eV. There is a large discrepancy in the results of DFT (-0.3 eV) and EAM (+0.08 eV) for $n = 4$, but this discrepancy has no significant effect on the analysis in this work. For the VH clusters, the EAM potential predicts $E_{VH}^b = 0.537$ eV as compared to the the DFT value of $E_{VH}^b = 0.62$. The binding energy of a divacancy is computed to be 0.14 eV using the EAM potential and 0.16 in DFT. The structures of the Fe edge dislocation as predicted by the QM/MM method and the EAM potentials are shown in Figure 2. The two structures are in very good agreement.

Table 1: Hydrogen-Vacancy-Dislocation interaction energies and barriers as calculated via DFT, QM/MM, and EAM methods

	Stand alone DFT	QM/MM	EAM
E_V^f (eV)	2.17	-	1.73
E_{VH}^b (eV)	0.62	-	0.537
E_{VV}^b (eV)	0.16	-	0.14
E_{d-V}^{int} (eV)	-	-1.47	-1.08
Max E_{d-H}^b (eV)	-	0.47	0.37
E_{V-d}^m (eV)	-	0.14	0.1
E_{V-H}^b (eV)	-	1.617	1.677
E_{d-VH}^m (eV)	-	-	0.58

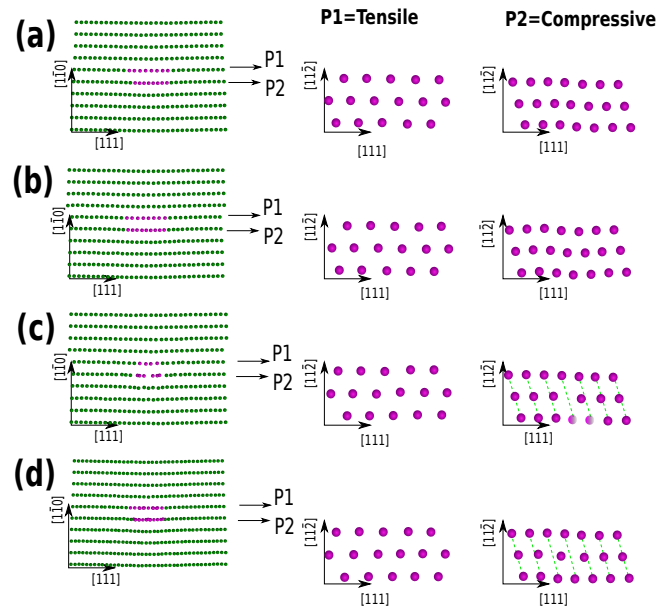


Figure 2: Atomistic structure of an edge dislocation core in Fe as computed by (a) the EAM potential and (b) the QM/MM method. Blue symbols denote atoms in a local bcc environment and red symbols indicate all other atom environments. With a vacancy located on the first plane on the compressive side of the glide plane, and in the middle of the core, the computed structures are computed as (c) the QM/MM method and (d) the EAM potential [15].

In the presence of the dislocation, a Vacancy is placed in the center of the dislocation on the compressive side of the glide plane, where the Vacancy should be most favorable due to its negative misfit volume. The interaction energy E_{d-V}^{int} between this V and the edge dislocation is computed as

$$E_{d-V}^{\text{int}} = E_{d-V} - (E_d + E_{\text{Fe}}^{\text{coh}} + E_V^{\text{f}}) \quad (1)$$

where E_d is the energy of the system with just the dislocation, $E_{\text{Fe}}^{\text{coh}}$ is the bulk Fe cohesive energy, E_V^{f} is the bulk vacancy formation energy, and E_{d-V} is the energy of the system with the Vacancy in the dislocation core. The V/dislocation interaction energy is $E_{d-V}^{\text{int}} = -1.08$ eV for the EAM potential and -1.47 eV for the QM/MM method. The difference between EAM and QM/MM for the Vacancy in the core is thus nearly identical to the difference in formation energy. Thus, while the EAM predicts a rather weaker binding of the V to the dislocation core, the energy gain associated with Vacancy annihilation in the core (see below) is nearly the same for EAM and QM/MM. In spite of the similar trends in energy, the configuration of the V/dislocation system obtained by QM/MM and EAM calculations are quite different, as seen in Figure 2c. In the QM/MM model, the vacancy occupies a substitutional lattice position, with displacements of the surrounding Fe atoms toward the vacancy site. In contrast, in the EAM model the vacancy is shared by two atomic sites such that a single Fe atom sits in between two lattice sites.

Hydrogen/dislocation interactions have been previously studied using a related QM/MM method [28]. The largest interaction energy occurs for an H atom on the tensile side of the core, due to the positive misfit volume of H in the tetrahedral interstitial sites of the Fe lattice. The interaction energy at this site is -0.37 eV using the EAM potential as compared to -0.47 eV obtained from the QM/MM method. Thus, the EAM potential slightly underpredicts H binding to the core, but this difference will have limited effect on most results below. For an H atom on the compressive side of the core, the interaction is unfavorable with the EAM potential predicting an interaction energy of 0.118 eV.

4. Reactions of dislocations with Vacancy-Hydrogen clusters

We now address issues associated with moving dislocations interacting with a variety of vacancy/hydrogen clusters. For a single vacancy located ahead of the dislocation on the first plane on the compression side of the dislocation, the EAM potential predicts that the vacancy is indeed absorbed by the dislocation and transported along with it as reported in [17]. This behavior is unexpected, since the migration barrier for V in bulk Fe is 0.6 eV. However, the binding energy of a V in the core of the dislocation is quite large and the equilibrium position shows that the V is shared between two lattice sites, i.e. an Fe atom moves to a position in between two lattice sites (see Figure 2d). As a result of this local configuration, V migration in the glide direction can occur with a very low energy barrier. A Nudged Elastic Band calculation using the EAM potential at zero stress shows that

the migration barrier for V from the initial position to a neighboring position in the core is less than 0.1 eV, with the neighboring site have an energy only 0.08 eV larger. Thus, as the dislocation glides under the action of an applied stress, a V on the compressive side of the core can easily be dragged along with the dislocation. The QM/MM shows the same final result but with a different mechanism for transport of the single vacancy. When the vacancy is placed in the site neighboring the low energy site, the Vacancy is mechanical unstable and moves back to the central low-energy position. Thus, as the dislocation glides, the Vacancy follows relaxing into the (moving) low-energy site. When the dislocation glides by a single Burger's vector, the vacancy diffuses to the next atomic site to restore its original favorable position within the core. The NEB calculations show that the energy barrier for this diffusion process is 0.14 eV which is not significantly higher than that obtained from the EAM simulations. For both EAM and QM/MM, a single vacancy can be transported along with a gliding edge dislocation. However, this conclusion holds only for a Vacancy on the immediate compression plane below the glide plane. Both the EAM and QM/MM simulations show that a single vacancy in the second plane on the compression side of the dislocation, or on the first plane on the tension side, is not transported along with the dislocation. The binding energy and activation barrier away from the core, i.e. within a local bcc-like environment, does not allow for near-barrierless transport of the Vacancy. Therefore, the observation reported in [17] is limited to a single atomistic plane.

In the remainder of this section, we examine the interaction of vacancy and vacancy clusters with and without hydrogen by explicit EAM simulations. The strong binding of V in the core (~ 1 eV for this potential, ~ 1.47 eV for DFT) provides a high driving force for the V to remain associated with the dislocation core as it glides. However, when a single vacancy being transported by the dislocation encounters an H atom in the lattice, the V and H bind together and are not transported with the dislocation, i.e. the dislocation moves forward leaving behind the VH cluster as reported in [17]. The energetics of this process is unfavorable: the strongest binding of the VH cluster in the dislocation core is 1.617 eV, which is much larger than the energy 0.537 eV of the VH cluster in the bulk. Thus, the lack of transport is presumably a kinetic issue. An NEB calculation (EAM potential) of the motion of the V in the core with an H bound to the V in the initial position, but not to the final position, yields an activation barrier of 0.58 eV. This barrier prevents separation of the V from the H during dislocation glide. Dissociation of the VH cluster in the core is most favorable when the H is on the compression side of the glide plane, where it is unlikely to be found, and the H then migrates to the tensile side of the glide plane of the dislocation core.

With the VH cluster left behind a gliding dislocation, a second vacancy transported by a second dislocation to some positions near a previous VH cluster can bind to the VH to form a V_2H cluster. This cluster also remains behind as the second dislocation continues to glide. However, if this vacancy is in the atomic row adjacent to the VH cluster, the vacancies are annihilated and a double jog is formed, with the lone H atom left behind as the now-jogged dislocation continues to glide. Thus, the original VH cluster disappears entirely. This basic process establishes that stability of V-H clusters is easily defeated by vacancy annihilation and jog formation.

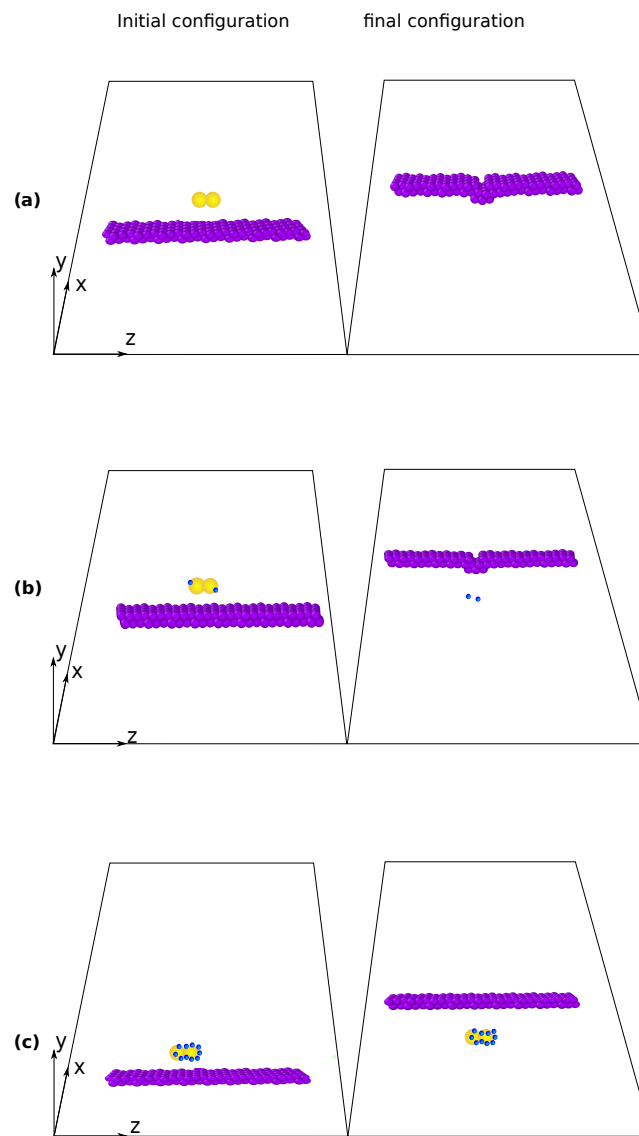
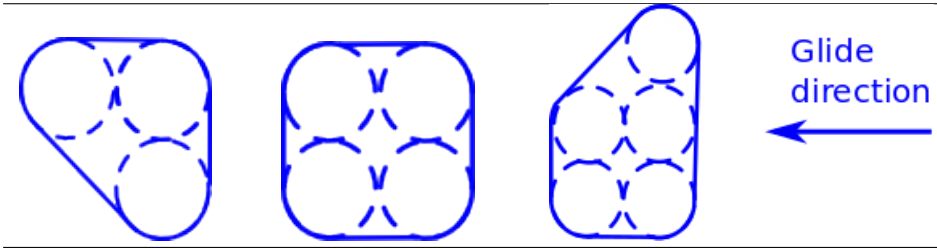


Figure 3: Interaction of an edge dislocation with (a) V_2 (b) V_2H_2 (c) V_2H_{10} clusters.

We now examine increasingly complex $V-H$ clusters. If a di-vacancy on the compressive side of the glide plane is oriented along the glide direction, the dislocation passes by without absorbing the vacancies. However, as shown in Fig. 3a, if the divacancy is oriented parallel to the dislocation line, the dislocation absorbs the two vacancies and forms a double jog. The same behavior is observed when a dislocation encounters a V_2H_2 cluster, as shown in Fig. 3b. For increasing H concentration in the divacancy, i.e. V_2H_n $n > 2$, vacancy annihilation and jog formation occur up to $n = 8$. For $n = 10, 12$, the H atoms stabilize the divacancy cluster. Thus, H atoms only stabilize divacancies at when the H content is very high. For larger planar V_mH_n ($m > 2$) clusters lying in the compressive plane below the glide plane, annihilation and jog formation remain dominant. For a compact tri-vacancy cluster $m = 3, n = 0$, a double jog forms and only one vacancy remains. For V_3H_3 , the same process occurs but with a VH_3 cluster left behind. For a tri-vacancy cluster with vacancies aligned in a single atomic row parallel to the dislocation line, all three vacancies are annihilated by the dislocation in both hydrogen free ($n = 0$) and hydrogen ($n = 3$) cases. If the tri-vacancy cluster is aligned perpendicular to the dislocation line, then there is no annihilation and the dislocation simply passes by the cluster, with or without hydrogen. Table 2 summarizes the processes associated with the interaction of larger planar vacancy clusters on the compressive side of the glide plane and the edge dislocation. Results show that, with or without hydrogen, two or more of the vacancies are always absorbed to form a double jog separated by a short edge segment on the glide plane below the original glide plane. The dislocation with the double-jog+climb defect continues to glide. The vacancy annihilation process is thus broadly favorable when there are at least two adjacent vacancies along the dislocation line direction, with or without hydrogen.

The processes observed above can be understood by examining the energetics of the reactions. Denoting a reaction that nucleates a double-jog as $V_nH_m + D \rightarrow V_{n-n'}H_m + DJ$ where DJ denotes a double jog, n' vacancies are annihilated. The change in total energy of the system is $-n'E_V^f + E_{V_nH_m}^b - E_{V_{n-n'}H_m} - 2E_J$,

Table 2: Reactions of an edge dislocation with various planar vacancy clusters, with and without hydrogen atoms. JD and D denote jogged and unjogged dislocations, respectively.



V_3	V_4	V_5
$V_3 + D \rightarrow JD + V$	$V_4 + D \rightarrow JD + V_2$	$V_5 + D \rightarrow JD + V$
$V_3H_1 + D \rightarrow JD + VH$	$V_4H + D \rightarrow JD + V_2H$	$V_5H_1 + D \rightarrow JD + V_2H$
$V_3H_2 + D \rightarrow JD + VH_2$	$V_4H_2 + D \rightarrow JD + V_2H_2$	$V_5H_2 + D \rightarrow JD + V_2H_2$
$V_3H_3 + D \rightarrow JD + VH_3$	$V_4H_3 + D \rightarrow JD + V_2H_3$	$V_5H_3 + D \rightarrow JD + V_2H_3$
-	$V_4H_4 + D \rightarrow JD + V_2H_4$	$V_5H_4 + D \rightarrow JD + V_2H_4$
-	-	$V_5H_5 + D \rightarrow JD + V_2H_5$

185 where $E_{V_nH_m}^b$ is the formation energy of a V_nH_m cluster relative to isolated V and H in the lattice and E_J is the jog formation energy. Since the vacancy formation energy is much larger, $\sim 1.7eV$, than the typical binding energies of V and H in clusters (at most $\sim 0.6 eV$), and the jog energy is not too large, the process of double-jog formation is usually energetically favorable even in the presence of hydrogen atoms. Annihilation of two vacancies decreases the energy by $\sim 3.4eV$ while the change in V-H interaction energies is typically only
 190 $\sim 1eV$. Only in the case where there are only two vacancies and $m = 10$ or more Hydrogens, such that the Hydrogen atoms return to the lattice after annihilation, is the V-H cluster stable.

Growing voids by the accumulation of vacancies is thus generally expected to be defeated by annihilation to form double jogs. To study this further, we imagine that V_mH_n clusters can diffuse and join to form larger nanovoids consisting of near-spherical clusters of vacancies, and analyze dislocation interactions with such
 195 nanovoids. We form equiaxed clusters of sizes $n = 9, 17, 25, 33, 41, 49$ with the center located on the compressive glide plane of an approaching dislocation. For all cases, the dislocation is pinned by the nanovoid, as expected. With increasing applied stress the dislocation bows out and eventually moves past the nanovoid. In all cases, the escape process is accompanied by double jog formation, as shown in Fig. 4 for a V_{49} nanovoid. In the jog formation process, the void loses the outermost vacancies on the compressive glide plane of the dislocation, and so the size of the cluster is reduced by the jog formation process. The behavior is not altered by the presence of Hydrogen. Specifically, for nanovoids of composition V_9H_{9n} , and $V_{25}H_{25n}$ with $n = 1, 2, \dots, 5$, the hydrogen atoms do not suppress annihilation and jog formation. For a much larger void of radius 17.5\AA , the dislocation is strongly pinned, escaping at $\tau = 650\text{MPa}$. With H atoms covering the void surface (H atoms at all near-tetrahedral sites on the void surface), the process is unchanged although the escape stress is reduced
 200 by 5%. While this suggests some possible hydrogen softening effect on the pinning strength of voids, that is not the focus here. The relevant conclusion from our analysis is that H does not stabilize voids or nanoclusters of
 205 vacancies against vacancy annihilation by the formation of double jogs.

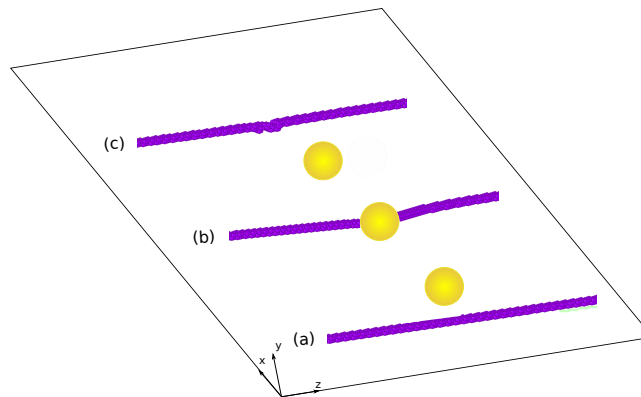


Figure 4: Interaction of an edge dislocation with a V_{49} cluster. (a) Prior to dislocation intersection; (b) during dislocation bow out under increasing stress; (c) after the dislocation is unpinned, showing the formation of a double jog.

5. Discussion

The process of void growth presented in [17] is based on several assumptions. First, single vacancies are swept along with dislocations. Second, these vacancies are pinned when they interact with an H atom, or a prior VH cluster, so that the vacancy transport process leads to sustained growth of vacancies clusters and voids. Third, hydrogen atoms stabilize the various vacancy clusters/voids. Our results confirm that the single vacancy transport process can occur, although the details of the process differ between the QM/MM and EAM simulations. However, both simulations confirm that this process is limited to vacancies only on the first plane on the compressive side of the glide plane. More importantly, our simulations show that vacancy clusters of two or more vacancies are most frequently reduced in size by vacancy annihilation and double-jog formation, with or without hydrogen. Only under conditions of very high hydrogen content in very small vacancy clusters can annihilation be prevented. Thus, the process proposed in [17] does not appear viable as an explanation for the observed nanovoids in Fe-based steel.

The annihilation process does contribute to the concentration of H into smaller vacancy clusters, but this process does not appear likely to allow growth of nanovoids. When an initial V_nH_m cluster is intersected by multiple dislocations, the vacancy annihilation process reduces the size to V_{n-n}/H_m so that the ratio H/V increases, stabilizing the smaller cluster. However, if the cluster grows again due to transport of single vacancies by dislocations, the growth of the cluster at fixed H leads to reduced stabilization, if not continued annihilation and reduction in the cluster size. As a specific case, when a V_4H_{10} cluster is struck by a dislocation and loses 2Vs, the V_2H_{10} cluster becomes stable against further annihilation. However, the addition of another single V creates a V_3H_{10} cluster, which is less stable. The V_3H_{10} cluster can then lose 2V by annihilation and double-jog formation to form a very stable VH_{10} . The VH_{10} cluster can then add one additional vacancy, but this simply returns the system to its original V_2H_{10} structure. Such cycles of growth, annihilation, and regrowth can thus occur, but cannot create large stable V-H clusters. Stabilization of vacancy clusters thus requires the separate process of H diffusion. Even with extensive H diffusion, the stable clusters would be very small (a few vacancies with very high H content). As we have seen, nanovoids with surfaces fully saturated with H are not stable against annihilation when dislocations intersect them.

The mechanism in [17] also involved growth of larger V-H nanovoids by void migration and coalescence. The results here show that larger V-H clusters are almost always less stable against subsequent annihilation via dislocation interactions. Void migration is also a rather slow process, and becomes slower with increasing H content [34]. Results in [17] show the migration barrier for VH to be ~ 0.7 eV, larger than that of a single vacancy ~ 0.6 eV, and much larger than that for H (~ 0.05 eV). Thus, it can be anticipated that single vacancies formed by plasticity processes can be quickly stabilized by the addition of one or more mobile H atoms, but then such clusters become far less mobile. This is likely what leads to the increase in V concentration in the presence of H as shown in the simulations shown in [17]. However, those simulations do not study the size of V or V-H clusters, and it is likely that the V remain isolated, i.e. no clusters formed are VH_m . Addition of more vacancies to a cluster further reduces the cluster mobility, and makes such cluster susceptible to annihilation processes unless there is significant H diffusion. H embrittlement in Fe is also observed at extremely low H concentrations, on the order of 1-10 ppm or less. Stabilization of the high (surface) density of nanovoids as observed in steels would, if H plays any role, require diffusion of H over extremely large volumes/distances.

A number of scenarios remain as possible explanations for the observed nanovoids. First, it is possible that VH clusters form, migrate, and coalesce, but with the migration moving them away from active slip planes such that intersections with dislocations, and thus annihilation, is infrequent. Second, the nanovoids are observed along grain boundaries, and it is possible that stabilization and diffusion of the VH cluster allows for VH diffusion to grain boundaries, leading to accumulation of V and H in the grain boundaries, with voids eventually being formed. The role of H in this process is unclear, however, since individual V could accomplish the same phenomenon, and with faster diffusion. In general, the high cost of forming vacancies in Fe (1.7 eV) implies that the equilibrium concentration is very low and that there is a strong driving force for almost any vacancy annihilation processes, suggesting that mechanisms relying on actual vacancy formation, stabilization, and migration are not likely. Third, H may (likely does) segregate rapidly to grain boundaries in Fe-based steels. The presence of H at the grain boundaries may inhibit dislocation transmission across grain boundaries, leading to accumulation of Burgers vector near the grain boundaries. This can, in turn, then lead to void nucleation at the grain boundaries, as observed in an entirely different system [35]. H could further stabilize such vacancies and limit their migration, leading to stabilization of small voids. We believe this last mechanism merits further investigation, and the weakening of grain boundaries by high densities of nanovoids can clearly favor cleavage-type failure processes along grain boundaries thus making a direct connection with embrittlement.

6. Conclusions

We have shown that QM/MM studies confirm that vacancies can be transported along with gliding edge dislocations in Fe, which is a surprising result. The transport of vacancies to pre-existing vacancy clusters,

with or without hydrogen, is thus possible. However, we show that, across many different types of vacancy clusters $V_n H_m$ with and without H, the annihilation of vacancies to form double-jogs on the dislocation is a dominating process. This is due to the large reduction of energy associated with vacancy annihilation. Therefore, the development of large V-H clusters by transport and trapping of vacancies is an unlikely phenomenon. The presence of sustained vacancy clusters/voids, while stabilized by H, must occur in spite of the annihilation processes caused by dislocations. The mechanism(s) associated with the observation of nanovoids at grain boundaries in Fe-based steels exposed to Hydrogen thus remain open, with several possible processes discussed briefly here.

Acknowledgments

AT and WAC gratefully acknowledge support of this work from the Swiss National Foundation through a grant for the project entitled “Predictive Mechanisms of Hydrogen Embrittlement” (project # 200021-149207).

References

- [1] R. Merrick, An overview of hydrogen damage to steels at low-temperatures, *Materials Performance* 28 (1989) 53.
- [2] P. R. Rhodes, L. A. Skogsberg, R. N. Tuttle, Pushing the limits of metals in corrosive oil and gas well environments, *Corrosion* 63 (2007) 63–100.
- [3] H. Rogers, Hydrogen embrittlement of metals atomic hydrogen from a variety of sources reduces the ductility of many metals, *Science* 159 (3819) (1968) 1057–1064.
- [4] J. C. Comer, The hydrogen economy: Opportunities, costs, barriers, and r&d needs., *Current Reviews for Academic Libraries* 42 (2005) 1053.
- [5] A. R. Troiano, The role of hydrogen and other interstitials in the mechanical behavior of metals, *trans. ASM* 52 (1) (1960) 54–80.
- [6] W. Gerberich, P. Marsh, J. Hoehn, Venkataraman, S., H. Huang, Hydrogen/ plasticity interactions in stress corrosion cracking, in: *Corrosion-Deformation Interactions (CDI'92)* editors: Magnin, T and Gras, J.M., 1993, pp. 325–353.
- [7] R. Oriani, P. Josephic, Equilibrium aspects of hydrogen-induced cracking of steels, *Acta Metallurgica* 22 (9) (1974) 1065–1074.
- [8] W. Gerberich, T. J. Foecke, Hydrogen enhanced decohesion in fe-si single crystals: implications to modeling of thresholds hydrogen effects on materials behavior, in: editors: Moody, N. R. and Thompson, A. W. (Warrendale, PA: TMS), 1990, pp. 687–701.
- [9] R. Oriani, A mechanistic theory of hydrogen embrittlement of steels, *Berichte der Bunsengesellschaft für physikalische Chemie* 76 (8) (1972) 848–857.
- [10] W. Gerberich, P. Marsh, J. Hoehn, Hydrogen induced cracking mechanisms—are there critical experiments?, *Hydrogen Effects in Materials* (1996) 539–554.
- [11] H. K. Birnbaum, P. Sofronis, Hydrogen-enhanced localized plasticity—a mechanism for hydrogen-related fracture, *Materials Science and Engineering: A* 176 (1) (1994) 191–202.
- [12] C. Beachem, A new model for hydrogen-assisted cracking (hydrogen “embrittlement”), *Metallurgical transactions* 3 (2) (1972) 441–455.
- [13] I. Robertson, The effect of hydrogen on dislocation dynamics, *Engineering Fracture Mechanics* 68 (6) (2001) 671–692.
- [14] J. Song, W. Curtin, A nanoscale mechanism of hydrogen embrittlement in metals, *Acta Materialia* 59 (4) (2011) 1557–1569.
- [15] J. Song, W. Curtin, Atomic mechanism and prediction of hydrogen embrittlement in iron, *Nature materials* 12 (2) (2013) 145–151.
- [16] T. Neeraj, R. Srinivasan, J. Li, Hydrogen embrittlement of ferritic steels: observations on deformation microstructure, nanoscale dimples and failure by nanovoiding, *Acta Materialia* 60 (13) (2012) 5160–5171.
- [17] S. Li, Y. Li, Y.-C. Lo, T. Neeraj, R. Srinivasan, X. Ding, J. Sun, L. Qi, P. Gumbsch, J. Li, The interaction of dislocations and hydrogen-vacancy complexes and its importance for deformation-induced proto nano-voids formation in α -fe, *International Journal of Plasticity* 74 (2015) 175–191.
- [18] H. D., D. J. Bacon, *Theory of dislocations*, Oxford Oxfordshire ; New York: Pergamon Press, 1984.
- [19] M. R. Hestenes, E. Stiefel, Methods of conjugate gradients for solving linear systems.
- [20] T. Schneider, E. Stoll, Molecular-dynamics study of a three-dimensional one-component model for distortive phase transitions, *Physical Review B* 17 (3) (1978) 1302–1322.
- [21] P. H. B. William C. Swope Hans C. Andersen, K. R. Wilson, A computer simulation method for the calculation of equilibrium constants for the formation of physical clusters of molecules: Application to small water clusters, *J. Chem. Phys.* 76 (1) (1982) 637–649. doi:10.1063/1.442716.
URL http://jcp.aip.org/resource/1/jcpsa6/v76/i1/p637_s1
- [22] S. Plimpton, Fast parallel algorithms for short-range molecular dynamics, *Journal of computational physics* 117 (1) (1995) 1–19.
- [23] A. Stukowski, Visualization and analysis of atomistic simulation data with ovito—the open visualization tool, *Modelling and Simulation in Materials Science and Engineering* 18 (1) (2009) 015012.
- [24] A. Ramasubramaniam, M. Itakura, E. A. Carter, Interatomic potentials for hydrogen in α -iron based on density functional theory, *Physical Review B* 79 (17) (2009) 174101.
- [25] X. Zhang, G. Lu, Quantum mechanics/molecular mechanics methodology for metals based on orbital-free density functional theory, *Physical Review B* 76 (24) (2007) 245111.
- [26] X. Zhang, C.-Y. Wang, G. Lu, Electronic structure analysis of self-consistent embedding theory for quantum/molecular mechanics simulations, *Physical Review B* 78 (23) (2008) 235119.
- [27] Y. Zhao, C. Wang, Q. Peng, G. Lu, Error analysis and applications of a general qm/mm approach, *Computational Materials Science* 50 (2) (2010) 714–719.
- [28] Y. Zhao, G. Lu, Qm/mm study of dislocation—hydrogen/helium interactions in α -fe, *Modelling and Simulation in Materials Science and Engineering* 19 (6) (2011) 065004.
- [29] G. Kresse, J. Hafner, Ab initio molecular dynamics for liquid metals, *Physical Review B* 47 (1) (1993) 558.

- [30] G. Kresse, J. Furthmüller, Efficient iterative schemes for ab initio total-energy calculations using a plane-wave basis set, *Physical Review B* 54 (16) (1996) 11169.
- 335 [31] J. P. Perdew, K. Burke, M. Ernzerhof, Generalized gradient approximation made simple, *Physical review letters* 77 (18) (1996) 3865.
- [32] H. J. Monkhorst, J. D. Pack, Special points for brillouin-zone integrations, *Physical Review B* 13 (12) (1976) 5188.
- [33] V. Shastry, D. Farkas, Molecular statics simulation of fracture in-iron, *Modelling and Simulation in Materials Science and Engineering* 4 (5) (1996) 473.
- 340 [34] Y. Wang, D. Connétable, D. Tanguy, Hydrogen influence on diffusion in nickel from first-principles calculations, *Physical Review B* 91 (9) (2015) 094106.
- [35] M. Dewald, W. Curtin, Multiscale modelling of dislocation/grain-boundary interactions: I. edge dislocations impinging on σ_{11} (1 1 3) tilt boundary in al, *Modelling and Simulation in Materials Science and Engineering* 15 (1) (2006) S193.